Journal of Solid State Chemistry 184 (2011) 1043–1047

Contents lists available at ScienceDirect

Journal of Solid State Chemistry

journal homepage: www.elsevier.com/locate/jssc

Preparation, crystal structures and rapid hydration of P2- and P3-type sodium chromium antimony oxides

A.A. Pospelov †, V.B. Nalbandyan *

Southern Federal University, 7 ul. Zorge, Rostov-na-Donu 344090, Russia

ARTICLE INFO

Article history:
Received 2 October 2010
Received in revised form
4 March 2011
Accepted 5 March 2011
Available online 15 March 2011

Keywords:
Layered structure
Prismatic coordination
Rietveld method
Chromite
Antimonate
Solid electrolyte

ABSTRACT

Two new $Na_x[Cr_{(1+x)/2}Sb_{(1-x)/2}]O_2$ compounds have been prepared by solid-state reactions in argon. Their structures have been determined by the X-ray Rietveld method. Both new phases together with $NaCrO_2$-based solid solution comprise brucite-like layers of edge-shared $(Cr,Sb)O_6$ octahedra but differ by packing mode of the layers and coordination of the interlayer Na^+ ions. A P3 phase exists at $x\approx 0.5$–0.58. It is rhombohedral ($R\bar{3}m$), $a=2.966$, $c=16.937$ Å at $x\approx 0.58$, with 29% Na^+ occupancy of trigonal prisms. A P2 phase exists at $x\approx 0.6$–0.7. It is hexagonal ($P6_3/mmc$), $a=2.960$, $c=11.190$ Å at $x\approx 0.7$, with 37% and 33% Na^+ occupancy of two non-equivalent trigonal prisms. Both P2 and P3 phases rapidly absorb moisture in air; packing mode is preserved, the a parameter changes slightly but c increases by 24–25%. Very high sodium ion conductivity is predicted for both P2 and P3 anhydrous phases.

1. Introduction

Nonstoichiometric mixed oxides $A_x(L,M)O_2$ (A=K, Na) based on brucite-like octahedral $[(L,M)O_{6/3}]^{x-}$ layers known as P2 and P3 types (for prismatic coordination of the alkali cations and number of layers in a hexagonal unit cell) are among the most conducting K^+ and Na^+ solid electrolytes [1–5]. Principles of their stability and crystal-chemistry factors responsible for high ionic conductivity have been discussed in several preceding reports [4–9] and a recent review [10]. Here, we report two new compounds of the same family with general formula $Na_x[Cr_{(1+x)/2}Sb_{(1-x)/2}]O_2$ promising even higher conductivities.

2. Experimental

Starting materials were reagent-grade sodium carbonate, ammonium dichromate and hydrous antimonic acid. Sodium carbonate was dried at 150 °C; antimonic acid was analyzed by weight loss on calcining to Sb_2O_4 and then used in its non-calcined air-dry form; active chromium oxide was prepared by "burning" the dichromate and further calcined at 300 °C to remove any traces of volatile components. The reagents were weighed in desired ratios, mixed thoroughly with a mortar and pestle, pressed into pellets and calcined in two or three steps, 1–3 h each, first at 730–750 °C, finally at 1000–1030 °C, with intermediate grinding and pressing.

X-ray diffraction studies were performed in Cu$K\alpha$ radiation using first a DRON-2.0 diffractometer with Ni filter, then a Rigaku D/Max-RC instrument with a secondary-beam graphite monochromator and, finally, an ARL X'TRA diffractometer equipped with an energy-dispersive Si(Li) detector.

In the system under study, chromium oxide is the most inert component, and it may stay unreacted after rapid interaction between the most basic and most acidic components, soda and antimonic acid, respectively. To prevent this two-component reaction and assist Cr_2O_3 binding, all antimony was introduced in the form of $CrSbO_4$, presynthesised at 1000 °C in air and verified by X-rays. Thus, the reaction mixtures were actually composed of Na_2CO_3, Cr_2O_3 and $CrSbO_4$. Empirically selected excesses of soda (usually 10–15% of the calculated amount) were introduced to compensate for high volatility of soda at the reaction temperatures. In addition, the pellets were covered with sacrificial powders of the same composition.

Syntheses of the triple oxides based on Cr(3+) could not be performed in air because Cr(3+) is easily oxidized to chromate in alkaline environment. On the other hand, we could not use reducing atmosphere, as in preparation of $Na_x(Cr_xTi_{1-x})O_2$ [4], because of unavoidable reduction of Sb(5+). Therefore, the preparations were carried out in inert atmosphere of flowing argon in a tubular furnace.

Selected preparations were analyzed by X-ray fluorescence using an Axios Advanced spectrometer (Philips Analytical) calibrated

* Corresponding author.
E-mail address: vbn@sfedu.ru (V.B. Nalbandyan).
† Perished in mountains on 11 February 2011.

0022-4596/$ - see front matter © 2011 Elsevier Inc. All rights reserved.
doi:10.1016/j.jssc.2011.03.011

vs. standard mixtures made with Na:Cr:Sb ratios close to those expected in the calcined samples.

Powder structure analyses were performed by the Rietveld method using the GSAS +EXPGUI suite [11,12] and ARL X'TRA scans. To avoid hydration in ambient air, the flat powdered samples were enclosed in a home-made semicylindrical sample holder [13,14] sealed with a Scotch tape; in addition, a piece of NaOH as a desiccant was attached to a side wall of the holder.

3. Results and discussion

3.1. Phase analyses and chemical Compositions

Phase analyses of the nominal $Na_x[Cr_{(1+x)/2}Sb_{(1-x)/2}]O_2$ samples reveal formation of three brucite-related layered phases. One of them, with largest values of *x*, was rhombohedral $NaCrO_2$-based solid solution of the O3 type with octahedral (or, to be correct, trigonal-antiprismatic) coordination of all ions. Two others showed X-ray patterns typical of P2 and P3 types. However, most preparations resulted in mixtures of these phases, often with Cr_2O_3 and/or $NaSbO_3$ due either to excessive soda loss at high temperatures and prolonged heat treatments or to kinetic hindrances at reduced temperatures and short heating periods. In addition, equilibrium homogeneity ranges of different phases might depend on temperature; therefore, it was necessary to use rapid quenching to prevent phase changes on slow cooling, but it was impossible with our preparations in inert atmosphere. As a result, only tentative homogeneity ranges of the phases have been established.

Phase analyses were further complicated by rapid hydration of the P2- and P3-type phases in ambient air. First X-ray scans of freshly ground samples showed usually anhydrous phases with a strong basal reflection at 15.7–15.8° (2Θ Cu$K\alpha$) but immediate repeated scans revealed rapid weakening of this reflection and appearance of new reflection(s) at lower angles. Similar results were obtained after several weeks' storage in the "sealed" holder without internal desiccant. Without protection from atmosphere, high-quality X-ray patterns of the anhydrous P2- and P3-type phases could not be obtained, and single-phase patterns [15] could only be taken after full hydration, when the 15.7–15.8° reflection vanished (Fig. 1). These patterns were completely indexed on hexagonal primitive (P2) or rhombohedral (P3) lattices with reasonably high figures of merit $F_{22}=39$ and $F_{24}=32$, respectively. Their a parameters are close to those of the anhydrous phases but their *c* are expanded by 24–25% (see Table 1). Water content in the hydrates was determined by weight loss on heating. However, crystallinity of these samples was seriously damaged by the dehydration and the resulting X-ray patterns were not suitable for structure analysis. This damage cannot be explained by oxidation on heating in air because similar results have been obtained after drying in vacuum.

X-ray fluorescent analyses of selected calcined samples verified that Sb/Cr ratios, within experimental accuracy of ca. 1%, were the same as in the starting mixtures; therefore, antimony loss might be neglected. On the other hand, Na/Cr ratio showed strong scatter even in standard mixtures and, thus, sodium content could not be determined with any reasonable accuracy. It was, therefore, postulated to correspond to the general formula $Na_x[Cr_{(1+x)/2}Sb_{(1-x)/2}]O_2$ based on electroneutrality principle because substantial concentration of vacancies in the rigid part of structure is improbable, as well as any deviation from the stable oxidation states of Cr(3+) and Sb(5+) in inert atmosphere of synthesis. The latter point was confirmed by bond lengths which were found to be in reasonable agreement with those expected from the ionic radii (see below). Any reduction of

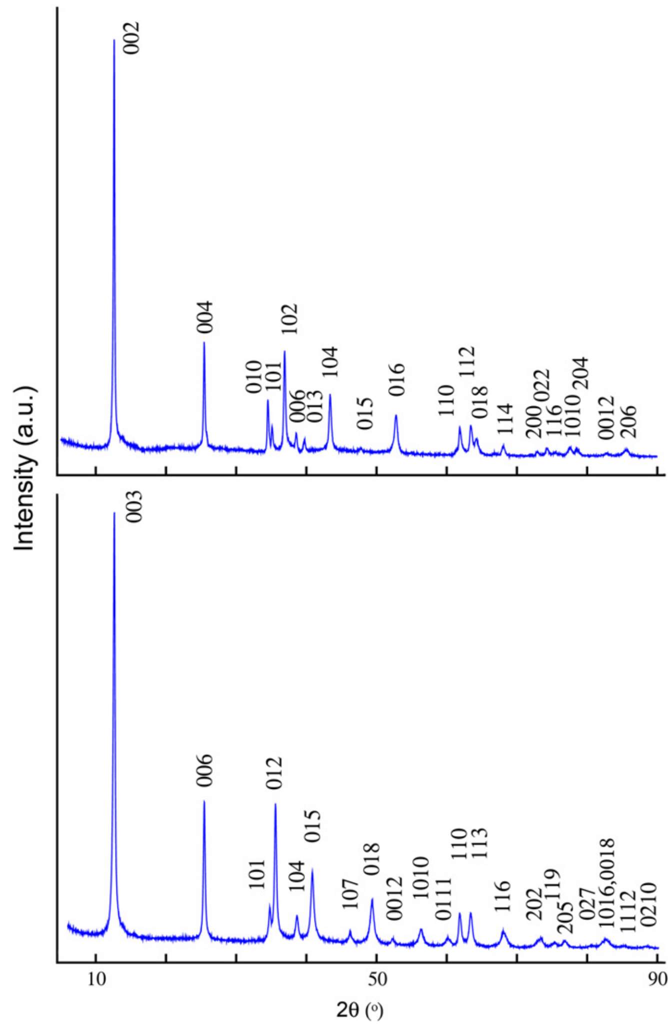

Fig. 1. X-ray powder diffraction patterns of fully hydrated P2-type $Na_{0.6}Cr_{0.8}Sb_{0.2}O_2$ $1.2H_2O$ (top) and P3-type $Na_{0.56}Cr_{0.78}Sb_{0.22}O_2$ $1.3H_2O$ (bottom).

Table 1
Compositions, lattice parameters and interlayer spacings d of sodium chromium antimony oxides.

Type	Formula	*a* (Å)	*c* (Å)	*d*=*c*/*n* (Å)
P3	$Na_{0.5}Cr_{0.75}Sb_{0.25}O_2$	2.965(2)	16.953(3)	5.651
	$Na_{0.56}Cr_{0.78}Sb_{0.22}O_2$	2.97	16.90	5.633
	$Na_{0.56}Cr_{0.78}Sb_{0.22}O_2$ 1.3 H_2O	3.0005(5)	21.0179(1)	7.006
	$Na_{0.58}Cr_{0.79}Sb_{0.21}O_2$	2.9631(5)	16.9287 (1)	5.643
P2	$Na_{0.6}Cr_{0.8}Sb_{0.2}O_2$	2.96	11.19	5.595
	$Na_{0.6}Cr_{0.8}Sb_{0.2}O_2$ 1.2 H_2O	2.9964(4)	13.9731(2)	6.987
	$Na_{0.7}Cr_{0.85}Sb_{0.15}O_2$	2.9595(5)	11.189(11)	5.595
O3	$NaCrO_2$ [16]	2.9739	15.968	5.323
	$NaCrO_2$ [17]	2.9747(1)	15.9538(3)	5.318

Sb(5+) would result in appearance of Sb(3+) which is much larger in size and, more important, never adopts regular octahedral coordination due to its stereochemically active lone pair of electrons. On the other hand, we cannot completely exclude possibility of partial room-temperature oxidation of Cr(3+) in air with sodium extraction in the form of NaOH.

Based on the overall volume of data, the following tentative homogeneity ranges at 1000–1030 °C have been proposed: $x\approx0.5$–0.58 for P3, $x\approx0.6$–0.7 for P2 and $x\approx0.8$–1.0 for O3. As evident from Table 1, all anhydrous phases have essentially the same a parameter because ionic radii of Cr(3+) and Sb(5+) differ by only 0.015 Å [18], but their interlayer distances increase with decrease in x from O3 to P2 and then to P3 due to O^{2-}–O^{2-} repulsion around sodium vacancies. This is a general feature of all similar systems [2–8].

Our attempt of preparing an analogous phase with Te(6+) instead of Sb(5+), "$Na_{0.61}Cr_{0.87}Te_{0.13}O_2$", proved unsuccessful. Reaction between Na_2CO_3, Cr_2O_3 and presynthesised Cr_2TeO_6 in argon resulted in formation of a molten chromate together with unknown phase(s) and unreacted Cr_2O_3. Since Cr(3+) is oxidized to Cr(6+), Te(6+) must be reduced: either spontaneously (with evolution of oxygen) or by Cr(3+) in alkaline environment, although these oxidation states are compatible in Cr_2TeO_6 (without alkali in air).

3.2. Crystal structures

Powder patterns of the two single-phase anhydrous samples (Figs. 2 and 3) have been successfully refined based on P2 and P3 models with reasonably low R-factors and χ^2 values (Table 2). For the P2-type sample, *hk*0 and 00*l* reflections are considerably narrower than reflections of general types *h*0*l* and *hkl*. This is, obviously, due to stacking faults, i.e., admixtures of triple-layered packings (P3 and/or O3). Therefore, besides structural and profile parameters, *hkl*-dependent broadening coefficients have been refined, resulting in significant lowering of the discrepancy factors. For the P3-type sample, *hkl*-dependent broadening is less pronounced, and it has been neglected during refinement.

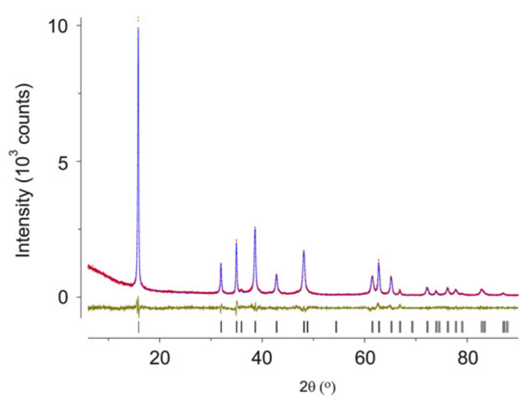

Fig. 2. X-ray diffraction pattern of P2-type $Na_{0.7}(Cr_{0.85}Sb_{0.15})O_2$. Points, experimental data; line, calculated profile; bottom, difference; vertical bars, Bragg positions.

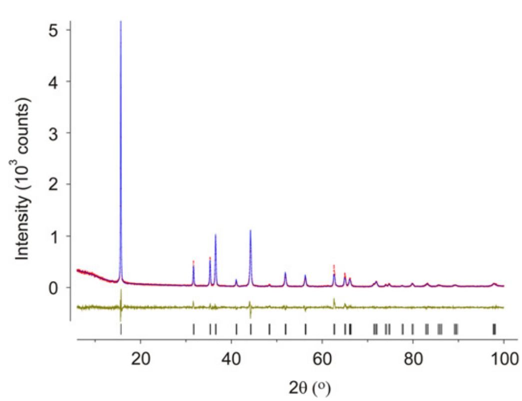

Fig. 3. X-ray diffraction pattern of P3-type $Na_{0.58}(Cr_{0.79}Sb_{0.21})O_2$. Points, experimental data; line, calculated profile; bottom, difference; vertical bars, Bragg positions.

Table 2
Crystallographic parameters, details of data collection and Rietveld refinement.

Formula	$Na_{0.7}Cr_{0.85}Sb_{0.15}O_2$	$Na_{0.58}Cr_{0.79}Sb_{0.21}O_2$
Crystal system	Hexagonal	Hexagonal
Space group	$P6_3/mmc$ (no. 194)	$R\bar{3}m$ (no. 166)
Lattice constants		
a (Å)	2.95982(8)	2.96620(7)
c (Å)	11.1903(7)	16.937(1)
Cell volume (Å^3)	84.90(1)	129.05(1)
Z	2	3
Density (calc.) (g/cm^3)	4.325	4.323
Wavelengths (Å)		
α1	1.5406	1.5406
α2	1.5444	1.5444
Ratio	0.5	0.5
2 Θ range (deg)	6.00–90.00	6.00–99.98
Step width (deg)	0.02	0.02
Count time (s)	3.6	2.0
No. of data points	4200	4700
No. of reflections	25	30
No. of parameters	35	27
Agreement factors		
R (F^2)	0.074	0.086
R_{wp}	0.093	0.129
χ^2	2.62	1.27

Table 3
Atomic coordinates, site occupancy factors and thermal displacement parameters of P2- and P3-type sodium chromium antimony oxides.

	x	y	z	s.o.f.	$U_{iso}\times 10^3$
$Na_{0.7}(Cr_{0.85}Sb_{0.15})O_2$ (P2)					
(Cr,Sb)	0	0	0	0.85/0.15	7.0(6)
O	1/3	2/3	0.0863(3)	1	6.8(13)
Na1	2/3	1/3	1/4	0.37(1)	17(5)
Na2	0	0	1/4	0.33(1)	120(10)
$Na_{0.58}(Cr_{0.79}Sb_{0.21})O_2$ (P3)					
(Cr,Sb)	0	0	0	0.79/0.21	15(1)
O	0	0	0.3917(2)	1	22(2)
Na	0	0	0.1668(6)	0.29	38(3)

Table 4
Principal interatomic distances (Å) and angles (deg) in P2- and P3-type sodium chromium antimony oxides.

Formula	$Na_{0.7}(Cr_{0.85}Sb_{0.15})O_2$	$Na_{0.58}(Cr_{0.79}Sb_{0.21})O_2$	Sum of radii [18]
Type	P2	P3	
(Cr,Sb)–O	1.963(2) × 6	1.977(2) × 6	2.00
(Cr,Sb)–O–(Cr,Sb)	97.9(1) × 3	97.2(1) × 3	
(Cr,Sb)–Na	2.7976(2) × 2	2.825(10) × 2	
Na1–O	2.505(3) × 6	2.508(8) × 3, 2.511(8) × 3	2.41
Na2–O	2.505(3) × 6		
Na–Na*	1.709 × 3	1.712 × 3	

* This is actually a distance between centers of the two adjacent prisms which cannot be occupied simultaneously. Without off-center displacements, actual Na–Na distances are equal either to the a parameter or to $2a/\sqrt{3}$. Displacements may make them somewhat longer.

Refined atomic coordinates, occupancies, thermal displacement parameters, principal interatomic distances and bond angles are listed in Tables 3 and 4. Both structures are illustrated in Fig. 4.

Attempts to locate water molecules in hydrates proved unsuccessful due to strong disorder, and also to small and very similar scattering factors of Na^+ and H_2O.

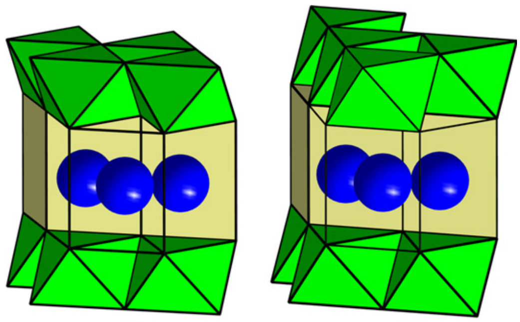

Fig. 4. Polyhedral presentation of P2 (left) and P3 (right) structures of sodium chromoantimonates. Part of the sodium prisms are open to show short distances between sodium sites which cannot be occupied simultaneously.

Table 5
Comparison of lattice parameters, interlayer O–O distances (common edges of NaO_6 prisms) and bottleneck radii *R* (half diagonal lengths of the prism faces) for several sodium-containing P2 and P3 phases.

Compound	Type	*a* (Å)	*c* (Å)	O–O (Å)	*R* (Å)	Hydration in air
$Na_{0.64}Ni_{0.32}Ti_{0.68}O_2$ [7]	P2	2.960	11.187	3.45	2.27	Slow
$Na_{0.66}Li_{0.22}Ti_{0.78}O_2$ [7,8]	P2	2.960	11.127	3.47	2.28	Slow
$Na_{0.74}Ni_{0.58}Sb_{0.42}O_2$ [9]	P2	3.012	11.226	3.51	2.31	Slow
$Na_{0.60}Cr_{0.60}Ti_{0.40}O_2$ [7]	P2	2.929	11.212	3.58	2.31	Slow
$Na_{0.70}Cr_{0.85}Sb_{0.15}O_2$	P2	2.960	11.190	3.66	2.355	Fast
$Na_{0.58}(Cr_{0.79}Sb_{0.21})O_2$	P3	2.966	16.937	3.67	2.36	Fast

Table 4 shows that average (Cr,Sb)–O bond lengths are in reasonable agreement with ionic radii sums; Na–O distances are slightly longer than the corresponding radii sum, and this is typical of partially occupied sites [18]. As in other brucite-related structures without metal–metal bonding, $(Cr,Sb)O_6$ octahedra are slightly flattened along the principal axis due to mutual repulsion of the polyvalent cations: the shared octahedral edges are contracted (corresponding bond angles are acute) whereas unshared edges, equal to the lattice constant *a*, are expanded (corresponding bond angles are obtuse).

Elevated thermal parameter of sodium ions (see Table 3) may be indication of their high mobility and/or their static off-center displacement forced by asymmetrical Na–Na repulsion [7,10] and/or their lower content due to either high-temperature volatilization or room-temperature topotactical oxidation in air, as discussed in Section 3.1. Due to strong correlation between site occupancies, thermal parameters and static displacements (position splitting), their independent determination from the powder X-ray data does not seem possible. In this study, sodium content was fixed to its nominal value, off-center displacements were not attempted and, therefore, only Na1/Na2 proportion in the P2 phase was refined with their sum occupancy fixed.

It was pointed out earlier [4–10] that the prismatic structures (P2 and P3) are stabilized with respect to O3 ($NaCrO_2$ or α-$NaFeO_2$ type) because they permit some Na^+–Na^+ distances to be longer than the cell edge *a* and, thus, to diminish the electrostatic repulsion, but this is only significant with relatively short *a*, not more than ~2.99 Å. This work provides one more confirmation for this idea: P2- and P3-type phases exist in the $Na_x[Cr_{(1+x)/2}Sb_{(1-x)/2}]O_2$ system with relatively small Cr(3+) ion and short $a \approx 2.96$–2.97 Å (Table 1), but do not exist in the analogous $Na_x[Fe_{(1+x)/2}Sb_{(1-x)/2}]O_2$ system with only slightly larger Fe^{3+} ($a \approx 3.02$ Å for the O3-type phase) [19]. These results also confirm that high electronegativity of the octahedral cations cannot be the main factor stabilizing prismatic structures [10], in contrast to the earlier suggestion [20], because Cr has lower electronegativity than Fe [21].

Comparison of the known sodium-containing P2- and P3-type structures (Table 5) shows, somewhat surprisingly, that, despite very similar lattice parameters, the new phases prepared in this work have considerably longer interlayer O–O distances and wider bottlenecks for sodium transport. This is manifested in their very fast hydration in air, similar to that of the potassium-containing P2- and P3-type phases [5], whereas other sodium-containing phases listed in Table 5 are relatively stable in air and absorb water slowly. It seems, therefore, that there is a critical O–O distance of ca. 3.6 Å, a border between "hard" and "easy" water intercalation.

The very wide bottlenecks, together with high concentration of sodium vacancies, very short intersite distances (jump distances) of 1.71 Å and high electronegativity of Sb^{5+} (thus, high ionicity of Na–O bonds), provide excellent conditions for high sodium ion conductivity, especially in hot-pressed grain-oriented ceramics. However, we did not succeed so far in preparing high-quality ceramic samples for direct measurements of conductivity because of the problems with phase purity, oxidation, and hydration.

4. Conclusions

Two new hexagonal phases based on brucite-like octahedral layers with trigonal-prismatic coordination of interlayer sodium ions have been prepared and characterized by full-profile X-ray structure analysis. It is confirmed that preference to trigonal prisms over antiprisms is mainly due to short value of the a parameter, determined by small sizes of Cr^{3+} and Sb^{5+}, rather than to high electronegativities of these cations. Both phases absorb atmospheric moisture rapidly with *c*-axis expansion of 24–25%. It is suggested that the interlayer O–O distances greater than 3.6 Å are responsible for this process because structurally related phases with slightly shorter O–O distances are relatively stable in air and intercalate water slowly. Very high sodium ion conductivity is predicted for the anhydrous materials.

Acknowledgments

The work was supported by the grant-in-aid 00-15 from the International Centre for Diffraction Data. The authors thank Dr. S.N. Polyakov for the Rigaku scans and O.E. Pustovit for the XRF analyses.

Appendix A. Supporting information

Supplementary data associated with this article can be found in the online version at doi:10.1016/j.jssc.2011.03.011.

References

[1] C. Delmas, C. Fouassier, J.-M. Reau, P. Hagenmuller, Mater. Res. Bull. 11 (1976) 1081–1086.
[2] A. Maazaz, C. Delmas, C. Fouassier, J.-M. Reau, P. Hagenmuller, Mater. Res. Bull. 14 (1979) 193–199.
[3] V.B. Nalbandyan, I.L. Shukaev, Russ. J. Inorg. Chem. 37 (1992) 1231–1235.
[4] M.Yu. Avdeev, V.B. Nalbandyan, B.S. Medvedev, Inorg. Mater. 33 (1997) 500–503.
[5] O.A. Smirnova, V.B. Nalbandyan, M. Avdeev, L.I. Medvedeva, B.S. Medvedev, V.V. Kharton, F.M.B. Marques, J. Solid State Chem. 178 (2005) 172–179.
[6] V.B. Nalbandyan, L.I. Medvedeva, T.I. Ivleva, Rus. J. Inorg. Chem. 40 (1995) 386–391.

[7] M.Yu. Avdeev, V.B. Nalbandyan, A.I. Beskrovnyi, in: Sixth European Powder Diffraction Conference (EPDIC-6), Budapest, Hungary, August 22–25, 1998, Scientific Program and Book of Abstracts, p. 235.
[8] G.V. Shilov, V.B. Nalbandyan, V.A. Volochaev, L.O. Atovmyan, Int. J. Inorg. Mater. 2 (2000) 443–449.
[9] O.A. Smirnova, M. Avdeev, V.B. Nalbandyan, V.V. Kharton, F.M.B. Marques, Mater Res. Bull. 41 (2006) 1056–1062.
[10] M. Avdeev, V.B. Nalbandyan, I.L. Shukaev, in: V.V. Kharton (Ed.), Solid State Electrochemistry I, Wiley-VCH, Weinheim, 2009, pp. 227–278.
[11] A.C. Larson, R.B. VonDreele, General Structure Analysis System (GSAS), Los Alamos National Laboratory Report LAUR 86-748, 2004.
[12] B.H. Toby, J. Appl. Cryst. 34 (2001) 210–213.
[13] N.G. Sudorgin, V.B. Nalbandyan, Elektrokhimiya 28 (1992) 122–124 in Russian.
[14] N.G. Sudorgin, V.B. Nalbandyan, I.L. Shukaev, Solid State Ionics 179 (2008) 503–507.
[15] S. Kabekkodu (Ed.), Powder Diffraction File, International Centre for Diffraction Data, 2009, cards 00-59-539 and 00-59-540.
[16] S. Kabekkodu (Ed.), Powder Diffraction File, International Centre for Diffraction Data, 2007, card 00-25-819.
[17] W. Scheld, R. Hoppe, Z. anorg, allgem. Chem. 568 (1989) 151–156.
[18] R.D. Shannon, Acta Cryst. A32 (1976) 751–767.
[19] V.V. Politaev, V.B. Nalbandyan, Solid State Sci. 11 (2009) 144–150.
[20] C. Delmas, C. Fouassier, P. Hagenmuller, Mater. Res. Bull. 11 (1976) 1483–1488.
[21] J. Emsley, The Elements, Clarendon Press, Oxford, 1991 (Russian translation, Mir, Moscow, 1993).